Electrodeposition of Platinum Metal and Platinum-Rhodium Alloy on Titanium Substrates

A. Baraka, H.H. Shaarawy, and H.A. Hamed

(Submitted 2 April 2002; in revised form 3 June 2002)

A method for application of an adherent platinum (Pt) and platinum-rhodium (Pt-Rh) alloy plate to a titanium (Ti) substrate includes steps of surface pretreatment, anodization, and electrodeposition of Pt and Pt-Rh alloy from their electrolytic baths consisting of $H_2Pt_2Cl_6 \cdot 6H_2O$ (20 gL^{-1}), and HCl (300 gL^{-1}) for a Pt bath. The Pt-Rh bath consists of $H_2Pt_2Cl_6 \cdot 6H_2O$ (20 gL^{-1}), and HCl (300 gL^{-1}) and $Rh_2(SO_4)_3$ (2 gL^{-1}). At the optimum conditions of electroplating, the Pt and Pt-Rh deposits were formed over the anodized Ti substrates with high adhesion, brightness, and high current efficiency (35.33% for Pt and 70.38% for the Pt-Rh alloy).

Keywords alloys, anodization, electrodeposition, platinum, rhodium, titanium

1. Introduction

Presently, there is substantial interest in noble metal plating, particularly because it is seen as a replacement for gold as a contact metal in the electronics industry. Several electrodeposition baths for palladium are commercially available, and their performances have been compared.[1-7]

Titanium (Ti) is a leading candidate material suitable for use in fabricating jet engine parts and other aircraft and aerospace components because it has high specific strength (yield stress/density) and resistance to corrosion.[8] Various methods can be used for application of metallic coatings on the Ti substrates.[9]

The formation of IrO_2/TiO_2 mixed oxide films supported on Ti metal plate was examined by Kristof et al.[10] The film is formed by thermal decomposition of Ti diisoperoxide bis-2, 4-pentanedionate in the presence of hydrated iridium (III) chlo-

A. Baraka and **H.A. Hamed,** Chemistry Department, Faculty of Science, Cairo University, Egypt; **H.H. Shaarawy,** Chemical Eng. & Pilot Plant, National Research Centre (NRC), Egypt. Contact e-mail: hosamnazer@hotmail.com.

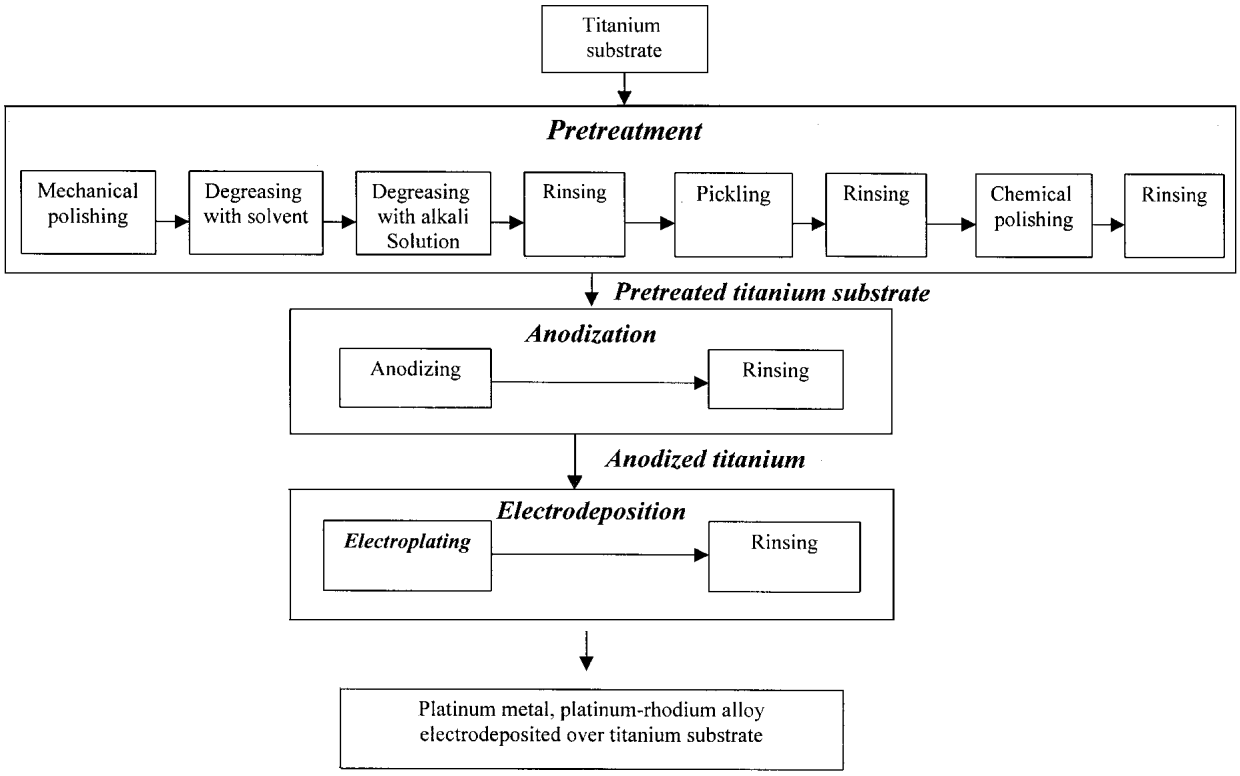

Fig. 1 Block flow diagram for the electrodeposition of Pt metal and Pt-Rh alloy over a titanium substrate

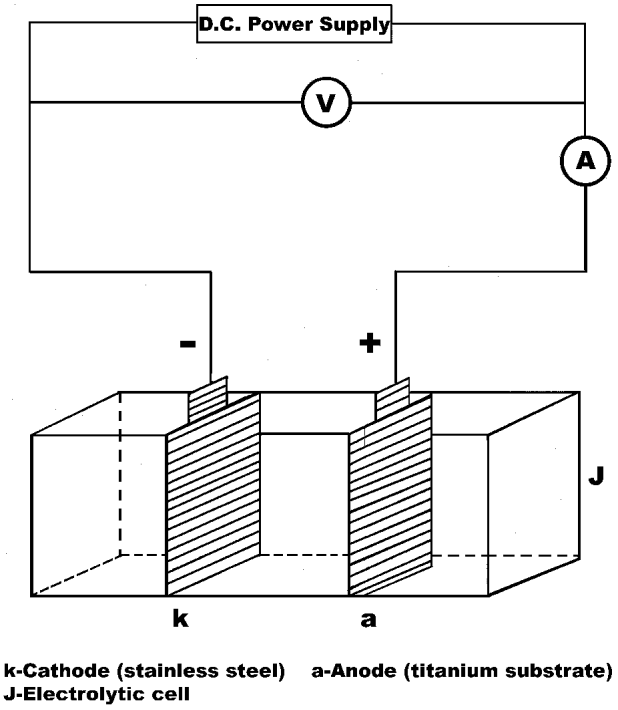

Fig. 2 Circuit diagram for the anodization process of Ti substrates

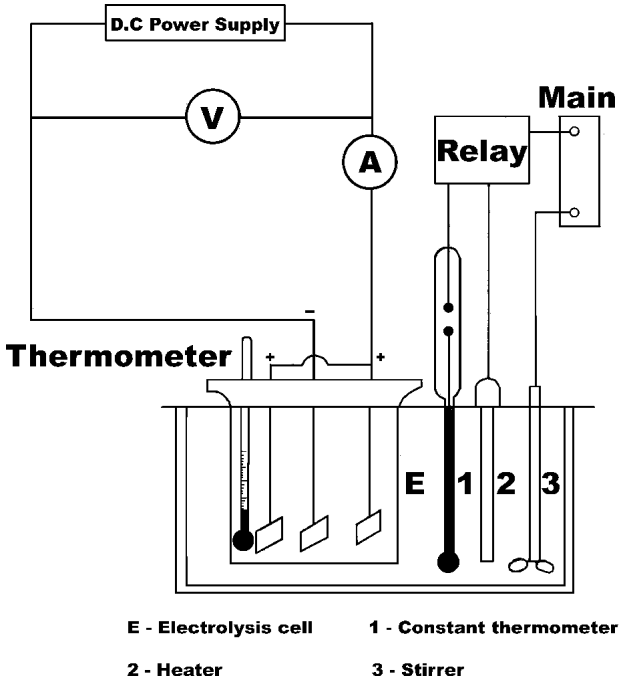

Fig. 3 Circuit diagram for the electrodeposition and current efficiency measurements

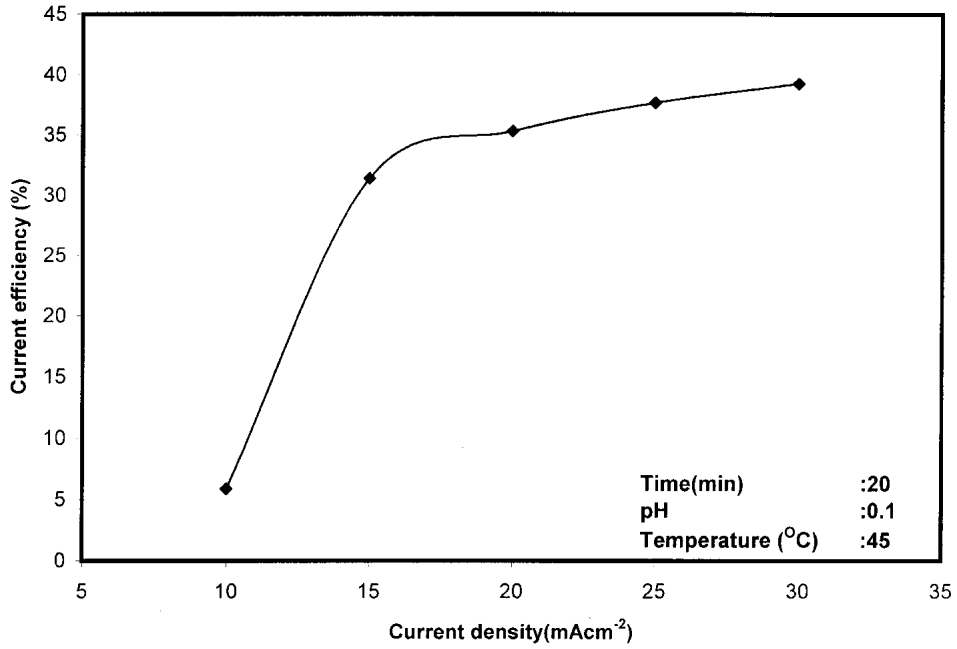

Fig. 4 Effect of current density on the current efficiency for the electrodeposition of Pt over a Ti substrate

ride solution. Different types of metal oxide coated electrodes, such as TiO_2, V_2O_5, Nb_2O_5, MnO_2, RnO_2, IrO_2, SnO_2, PbO_2, etc., were successfully fabricated[10-18]; some of these metal oxide coated electrodes are applied in real electrochemical processes such as saline electrolysis, production of alkali chloride, treatment or recycling of metal-containing wastewater, electrochemical synthesis of organic compounds, and decomposition of organic compounds.

The surface properties of ($Ru_{0.3}Pt_{0.4}$ $Ti_{0.3}O_x$) prepared by thermal decomposition of the respective chlorides on Ti in the temperature range 400-600 °C were studied by x-ray photoelectron spectroscopy (XPS), auger electron spectros-

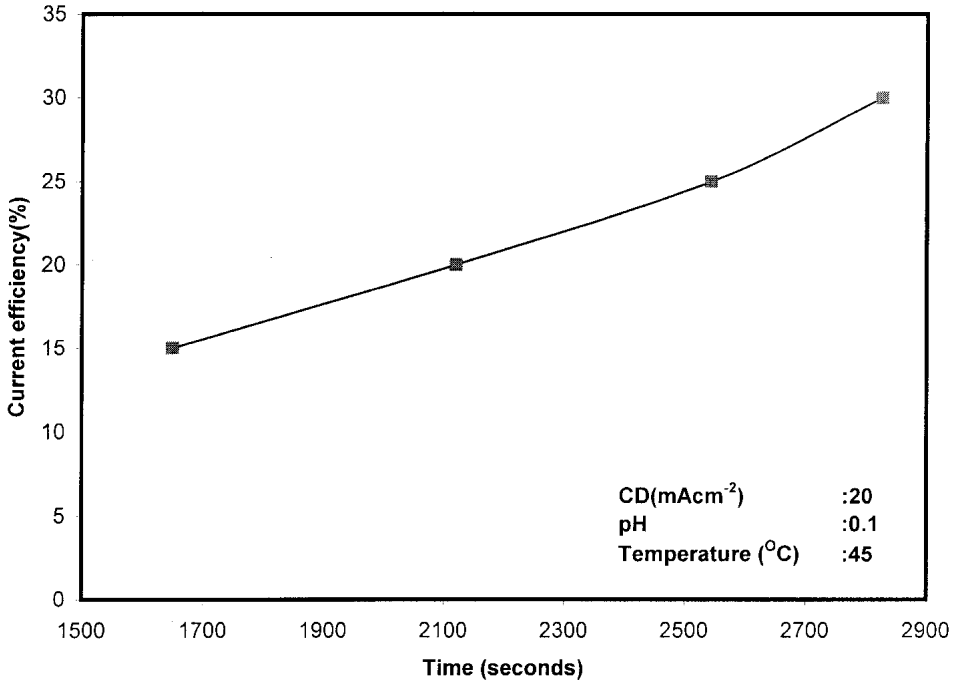

Fig. 5 Effect of time on the current efficiency for the electrodeposition of Pt over Ti substrate

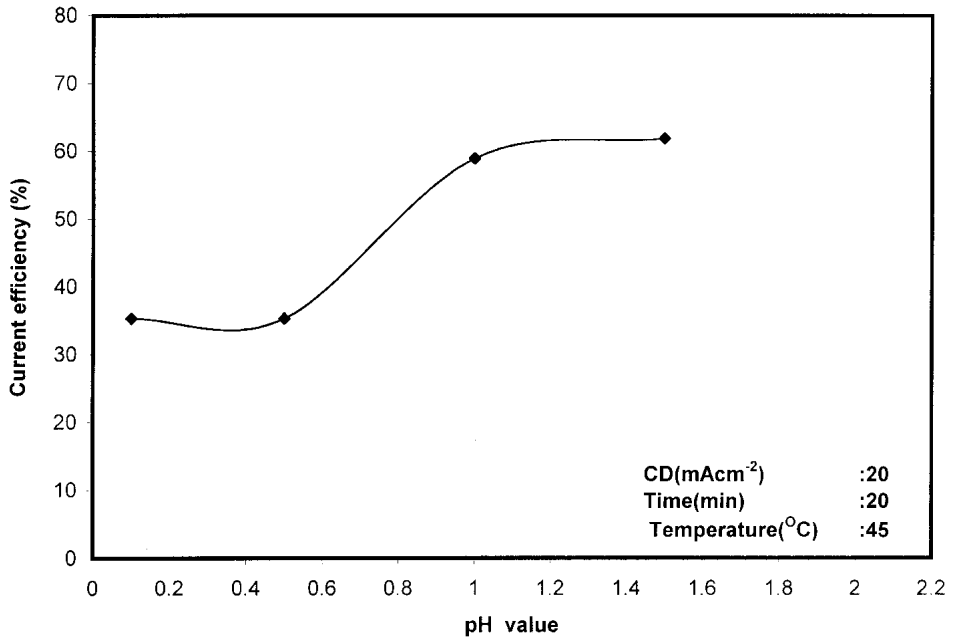

Fig. 6 Effect of pH on the current efficiency for the electrodeposition of Pt over a Ti substrate

copy (AES), and cyclic voltammetry in 1 M $HClO_4$ solution.[19-21]

In the present investigation, studies were carried out using electrochemical methods and an advanced technique for deposition of Pt and Pt-Rh alloy on Ti substrates. The process proceeded via surface pretreatment, anodization, and electrodeposition.[22]

2. Experimental

Figure 1 represents a process block flow diagram for the electrodeposition of the noble metals on a Ti substrate. Figure 2 shows the circuit diagram used for Ti anodization, and Fig. 3 represents the circuit diagram for electrodeposition and current efficiency measurements. Prior to the electrodeposition of pal-

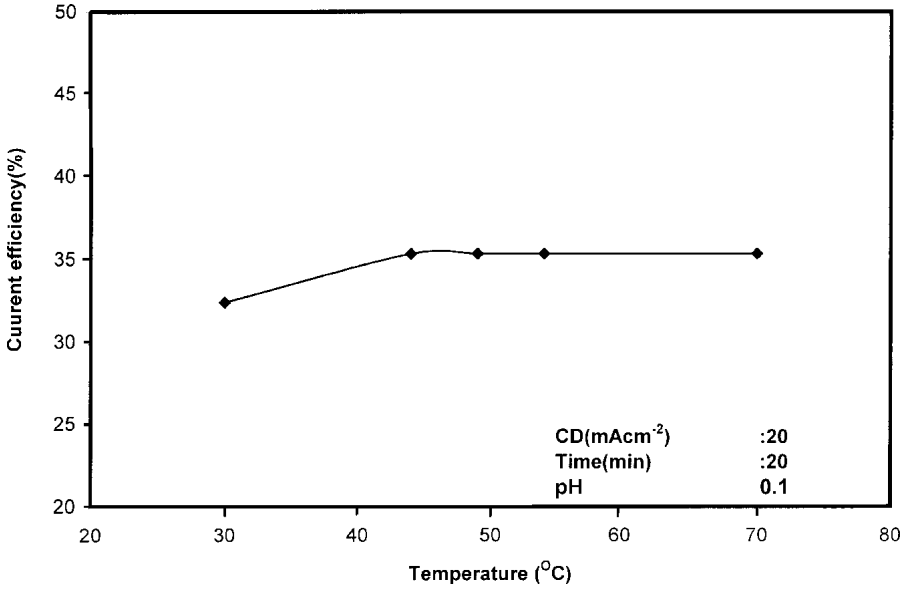

Fig. 7 Effect of electrolysis bath temperature on the current efficiency for the electrodeposition of Pt over a Ti substrate

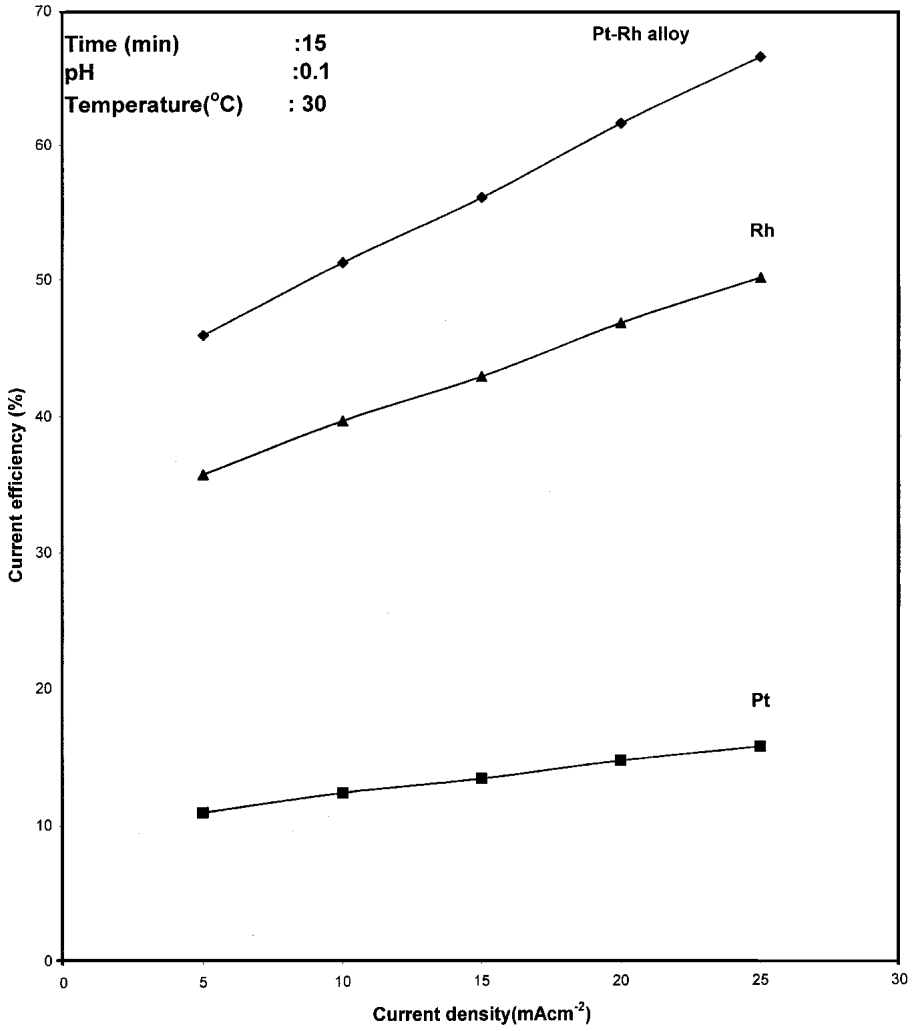

Fig. 8 Effect of current density on the current efficiency for the electrodeposition of Pt-Rh over a Ti substrate

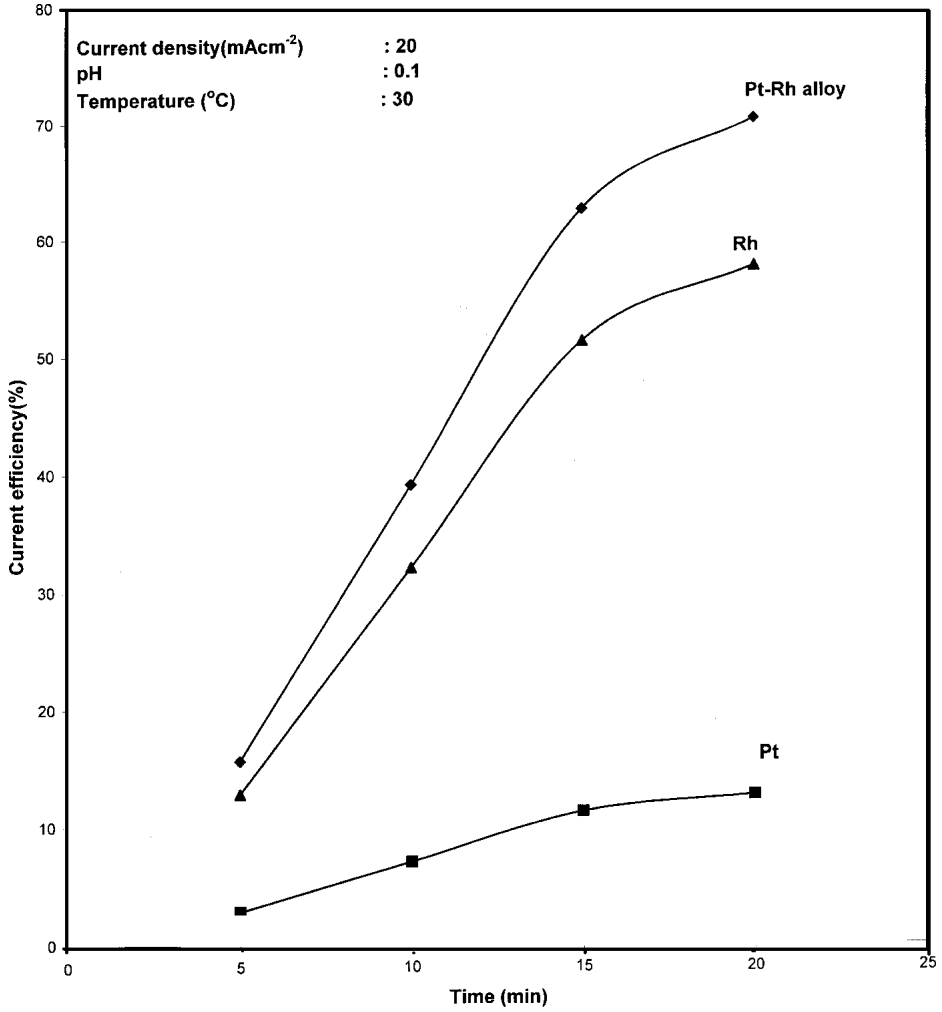

Fig. 9 Effect of time on the current efficiency for the electrodeposition of Pt-Rh alloy over a Ti substrate

ladium, the Ti substrates (IMI 115) of dimensions 1 × 1.4 cm^2 were pretreated by mechanical polishing, using sandpapers down to 4/0 grade, and degreasing with acetone. After this, the substrates were degreased in an alkali soaking cleaner of the following composition: NaOH 50 gL^{-1}, Na_2CO_3 20 gL^{-1}, Na_3PO_4 20 gL^{-1}, and sulphonic acid 2 gL^{-1}.[23-25] The degreasing process was carried out at 50 °C for 5 min, and then the Ti substrates were washed in running distilled water. The degreasing process was followed by pickling, where the substrates were immersed in a solution containing nitric acid (400 gL^{-1}) and hydrofluoric acid (50 gL^{-1}). This was found to be a good pickling solution, because it removed the oxides and scales from the Ti surfaces without difficulty and rendered the metal active. Finally, chemical polishing was carried out on the Ti substrates by their immersion and boiling in oxalic acid solution (100 gL^{-1}) for 5 min. The anodizing process was carried out on the pretreated Ti substrates in oxalic acid solution (80-100 gL^{-1}) at current density ranging from 15-25 mA cm^{-2}, at ambient temperature. These high current densities were chosen with the aim of obtaining porous and conductive Ti oxides on the surface of the substrates. Stainless steel electrodes (austenitic) were used as cathodes. The distance between the cathode and the anode was 2 cm.

The optimum composition of the Pt electroplating bath is $H_2Pt_2Cl_6 \cdot 6H_2O$ (20 gL^{-1}), and HCl (300 gL^{-1}) for the Pt bath. The Pt-Rh bath consists of $H_2Pt_2Cl_6 \cdot 6H_2O$ (20 gL^{-1}), HCl (300 gL^{-1}), and $Rh_2(SO_4)_3$ (2 gL^{-1}).[26]

The current efficiency of the electrodeposition process was calculated by Faraday's law.[27] The surface morphology and structure of the plated Ti were examined using a scanning electron microscope (SEM) JEOL (Tokyo, Japan) JSM T330A equipped with KEVEX (Tokyo, Japan) electron diffraction equipped (EDAX) x-ray microanalyzer. The operating conditions were accelerating voltage of 25 KeV, beam/sample incidence angle of 90°, and x-ray window incidence angle of 22.7°.

The phases and crystal structure of the deposited Pt and Pt-Rh alloy on the pre-anodized Ti substrates were examined by x-ray diffraction (XRD). The measurements were carried out using a Philips (USA) diffractometer (40 kV, 30 mA) with a nickel filter and copper radiation. The scanning angular range was from 4-90°. The diffraction pattern was recorded at room temperature.

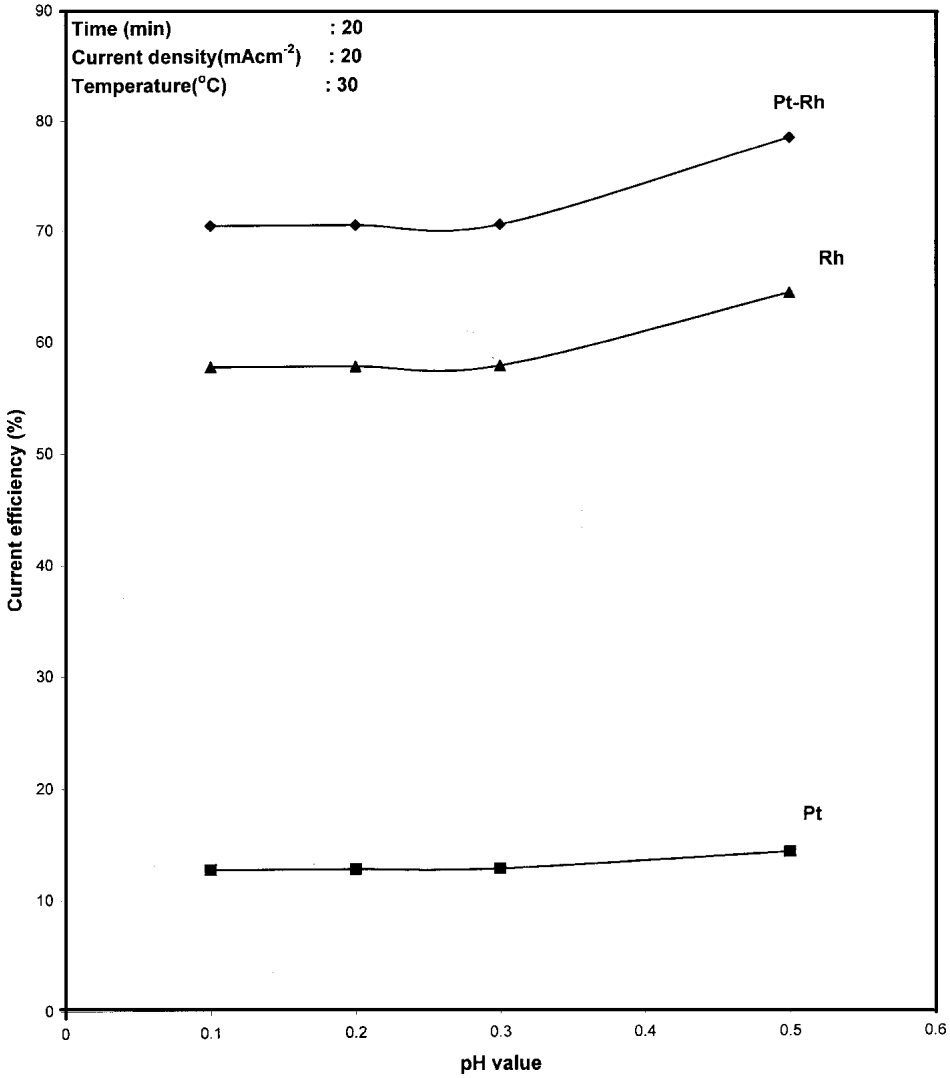

Fig. 10 Effect of pH on the current efficiency for the electrodeposition of Pt-Rh over a Ti substrate

3. Results

Figures 4-7 represent, respectively, the effect of applied current density, time of electrodeposion, pH, and temperature on the current efficiency of the electrodeposition of Pt over pre-anodized Ti substrates. Inspection of the results of these figures reveals that at pH of 0.1, temperature of 45 °C, and processing time of 20 min, the current efficiency increased with increasing applied current density from 10-30 mA cm^{-2}. At current densities higher than 20 mA cm^{-2} the formation of a "burnt" deposit occurred (Fig. 4). At a current density of 20 mA cm^{-2}, pH of 0.1, and temperature of 45 °C, the current efficiency increased with time from 15-30 min. At a time longer than 20 min, the formation of weak adherent deposits occurred (Fig. 5). At current density of 20 mA cm^{-2}, temperature of 45 °C, and time of 20 min, it was observed that the current efficiency slightly increased with increasing pH value of the bath from 0.1-0.5. At higher pH values, the stability of the bath decreased, and the formation of burnt deposits occurred (Fig. 6). At current density of 20 mA cm^{-2}, pH of 0.1, and time of 20 min, the change of temperature from 30-70 °C had a negligible effect on the current efficiency (Fig. 7). From the obtained results, it can be concluded that the more suitable conditions necessary to produce good adherent Pt deposits from the electrolytic bath may be current density of 20 mA cm^{-2}, time of 20 min, pH of 0.1, and temperature of 30 ± 2 °C. At these conditions the current efficiency was 35.33%.

Figures 8-11 represent the effect of applied current density, time of electrodeposition, pH, and temperature, respectively, on the current efficiency of the electrodeposition of Pt-Rh alloy over pre-anodized Ti substrates. The obtained results indicate that, at pH of 0.1, time of 15 min, and temperature of 30 °C, the current efficiency increases with increasing current density from 5-25 mA cm^{-2}. At current densities higher than 20 mA cm^{-2}, the formation of burnt multilayers of Pt-Rh deposits occurred (Fig. 8). At current density 20 mA cm^{-2}, pH of 0.1, and temperature of 30 °C, the current efficiency increases with increasing time from 5-20 min. At a more prolonged time, the

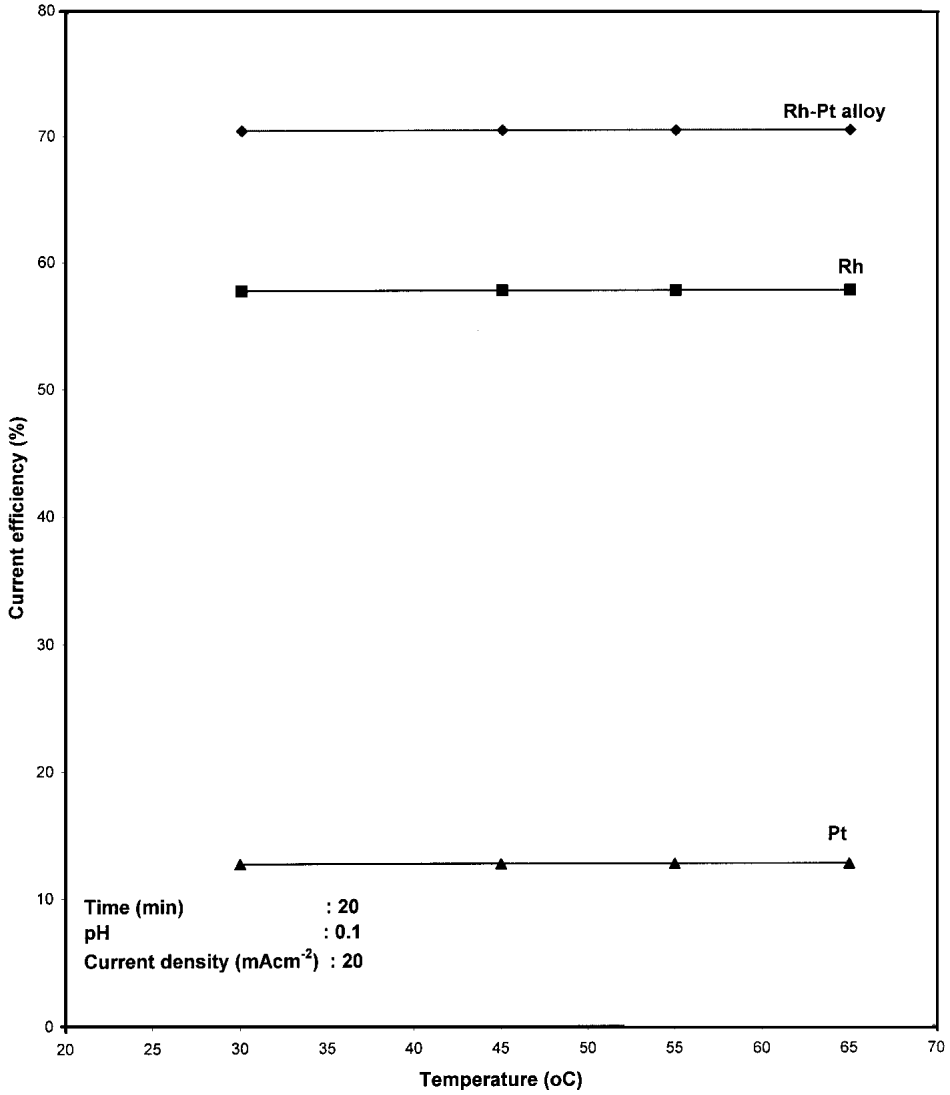

Fig. 11 Effect of temperature on the current efficiency for the electrodeposition of Pt-Rh over a Ti substrate

formation of nonadherent deposits on the Ti substrates occurred (Fig. 9). At current density 20 mA cm^{-2}, time of 20 min, and temperature of 30 °C, the current efficiency increases with increasing pH from 0.1-0.5. At pH values higher than 0.1, the formation of burnt deposits occurred (Fig. 10). At a current density of 20 mA cm^{-2}, pH of 0.1, and time of 20 min, the variation of temperature from 30-70 °C had no effect on the current efficiency. From the above-mentioned results, it can be concluded that the most suitable conditions for the electrodeposition of a Pt-Rh alloy over Ti substrates may be current density of 20 mA cm^{-2}, pH of 0.1, time of 20 min, and temperature of 30 °C. At these conditions the current efficiency reached 70.38%.

Figures 12-15 show, respectively, SEM-EDAX charts and photographs of morphology of the electrodeposited Pt metal and Pt-Rh alloy over the pre-anodized Ti substrates at the above-mentioned conditions. Deposits were in the form of large crystals, and many cracks with larger boundaries were obtained, which explained the presence of the Ti peak at 4.5 KeV for SEM-EDAX examinations. Figures 16-18 show the XRD pattern for anodized Ti substrates. The peaks in these figures were represented in terms of symbols where b stands for Pt, c stands for Rh, and d stands for Ti, the electrodeposited Pt metal and Pt-Rh alloy respectively, on these substrates. The identification of crystals is empirical; the American Society for Testing and Materials (ASTM) provides Keysort and IBM cards that provide d spacings and relative line intensities for pure compounds for over 25 000 crystalline materials. It is clear from the x-ray patterns that Pt metal and Pt-Rh alloy were electrodeposited on the pre-anodized Ti substrate, as shown from SEM-EDAX examinations. However, the presence of Ti peaks could mean that the noble metal films are very thin, perhaps ~1 μm.

4. Discussion

The electrodeposition of any metal or its alloy on the Ti substrates meets with many problems due to the formation of a

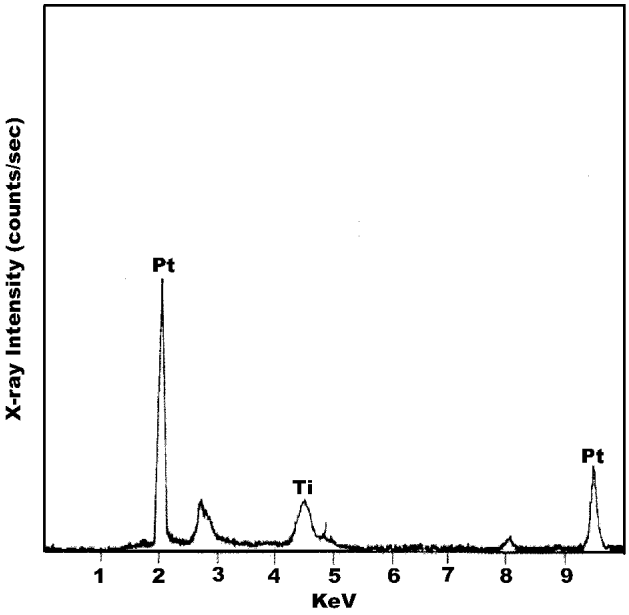

Fig. 12 SEM EDAC chart of the Pt/Ti electrode

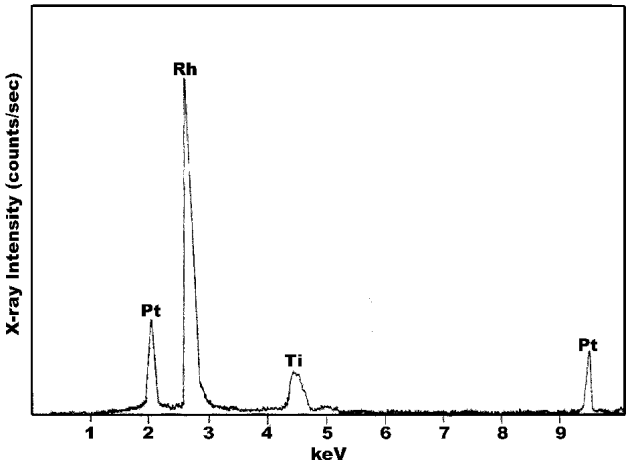

Fig. 13 SEM EDAX chart of the Pt-Rh/Ti electrode

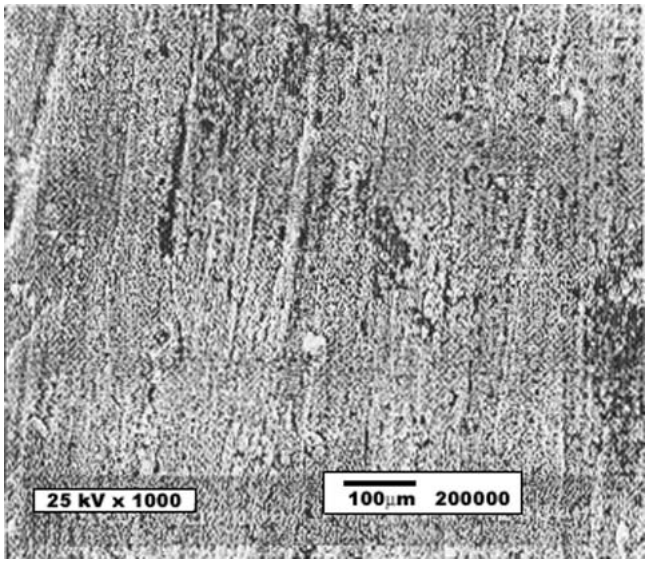

Fig. 14 SEM photograph showing a surface of the Pt/Ti electrode

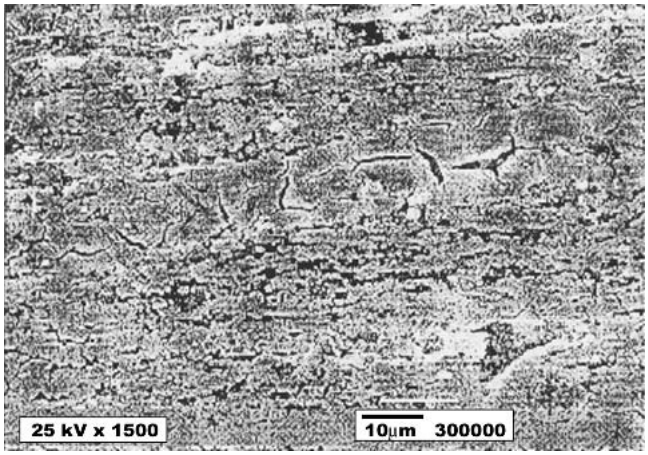

Fig. 15 SEM photograph showing a surface of the Pt-Rh/Ti electrode

nonconductive layer of Ti oxide on the surface of substrates during the electrodeposition process. Pre-anodization of Ti substrates at high current densities was carried out to overcome this problem.[22] At high current density, during the anodization of Ti, an anatase and rutile film is formed. Initially, this film reproduces perfectly on the Ti substrate; it is uniform, adherent, and seems to be grown epitaxially on the different grains of Ti substrate. As described previously by some researchers,[28] the kinetics of the oxide film growth depends on the crystallographic orientation of these grains. This growth of uniform film is limited at high current density by the breakdown of the films. The breakdown is accompanied by sparking, partial evaporation of the oxide, allotropic transformation of the low temperature stable anatase into the high temperature stable rutile and amorphous oxide, and finally by the formation of microporous films. Different interpretations published concerning the breakthrough on the anodic films formed on valve metals, are summarized in the publication of Albella et al.[29] This breakthrough is related to the injection of electrons from impurity centers to the oxide conduction band and avalanche multiplication of the electrons.[30] These impurity centers may be impurities of the metal substrate or electrolyte species incorporated in the anodic films, and the injected electrons resulting from these impurity centers may be responsible for the conductivity of the Ti oxide films (i.e., oxide film grafting or doping with electrons). The conductivity of these oxide films makes the anodized Ti substrate accessible for plating by the electrodeposition process.

The electrodeposition of Pt and Pt-Rh alloy on pre-anodized Ti substrates provides a process for obtaining a coated electrode having a good adhesion between the coating materials (Pt, Pt-Rh) and Ti substrates, and excellent electrochemical stability, and may lead to a superior catalytic activity in an acidic environment. The data obtained from Fig. 4-11 showed that the most effective conditions for the electrodeposition of Pt

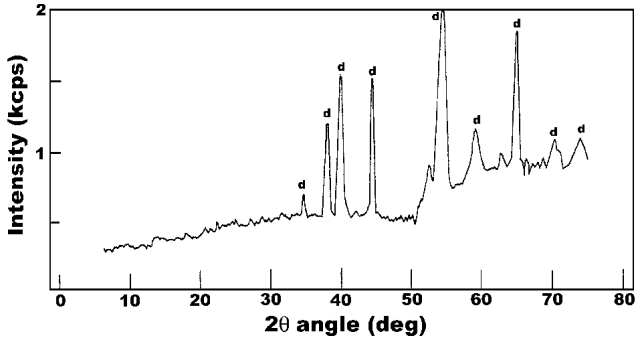

Fig. 16 XRD pattern for anodized Ti substrate

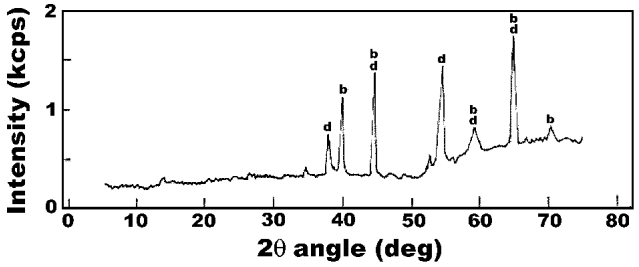

Fig. 17 XRD pattern for Pt/Ti electrode current density of 20 mA cm^{-2}, time of 20 min, pH of 0.1, and temperature of 30 ± 2 °C

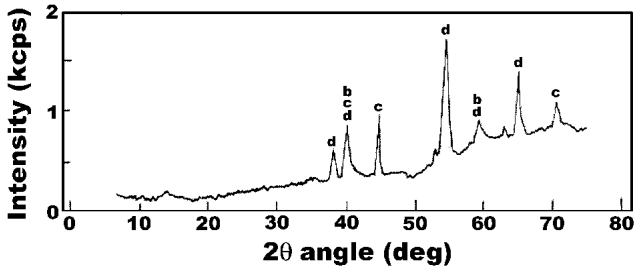

Fig. 18 XRD pattern for Pt-Rh/Ti electrode. Current density of 20 mA cm^{-2}, pH of 0.1, time of 20 min, and temperature of 30 °C

on Ti substrates were a current density of 20 mA cm^{-2}, time of 20 min, pH of 0.1, and temperature of 30 ± 2 °C, and for Pt-Rh alloy, a current density of 20 mA cm^{-2}, pH of 0.1, time of 20 min, and temperature of 30 °C. At these conditions, the current efficiency was 35.33% for Pt and 70.38% for Pt-Rh alloy.

5. Conclusion

Pt metal and Pt-Rh alloy were electrodeposited over the pre-anodized Ti substrates. The Pt and Pt-Rh deposits were formed with high adhesion, brightness, and high current efficiency (35.33% for Pt and 70.33% for the Pt-Rh alloy) from their electrolytic baths.

References

1. R.F. Vines, R.H. Atkinson, and F.H. Reid: in *Modern Electroplating,* F.A. Lowenheim, ed., Wiley, New York, 1974.
2. Ch.J. Raub: *Platinum Metals Rev.*, 1982, *26,* p. 198.
3. H.D. Hedrich and Ch. J. Raub: *Metalloberflache* (Germany), 1977, *31,* p. 512.
4. S. Jayakrishnan and S.R. Natarajan: *Metal Finishing,* 1988, *88,* p. 81.
5. D.M. Valle, F.R. Diaz, and H. Gome: *J. Appl. Electrochem.,* 1998, *28,* p. 943.
6. T. Christopher and D.S. Robert: *J. Am. Chem. Soc.,* 1996, *118,* p. 2634.
7. U. Kohei, Y. Shen, and N. Hideo: *J. Physical Chem. B,* 1997, *101,* p. 7566.
8. N. George: U.S. Patent No. 3 891 447, 1975.
9. D. Bernard: U.S. Patent No. 3 617 462, 1972.
10. H.B. Beer: U.S. Patent No. 3 711 385, 1973.
11. H.B. Beer: U.S. Patent No. 3 632 498, 1972.
12. B. Beden, F. Kadirgan, C. Lamy, and J.M. Leger: *J. Electroanal. Chem.,* 1981, *127,* p. 75.
13. R.R. Adzic, M.D. Spasojevic, and A.R. Despic: *J. Electroanal. Chem.,* 1978, *92,* p. 31.
14. A. Capon and R. Parsons: *Electroanal. Chem. Interfacial Electrochem.,* 1973, *45,* p. 205.
15. P. Con, B. Beden, H. Huser, and C. Lamy: *J. Electrochim. Acta,* 1987, *32*(3), p. 387.
16. L.E. Vaaler: *Electrothem. Technol.,* 1967, *5,* p. 170.
17. A. Visintin, W.E. Triaca, and A.J. Arvia: *J. Electroanal. Chem.,* 1990, *284,* p. 65.
18. H.C. Chung and W.T. Ching: *J. Electrochem. Soc.,* 1994, *141*(11), p. 2996.
19. A. Kar and J. Mazumder: *Metall. Trans. A,* 1989, *20A,* p. 363.
20. D. Michell, D.A.J. Rand, and R. Woods: *J. Electroanal. Chem.,* 1977, *89,* p. 117.
21. T. Lassali and R. Landers: *J. Electrochim. Acta,* 1999, *39,* p. 95.
22. H.A. Hamed: "Treatment of Industrial Wastewater Using Electrocatalytic Oxidation Technique," M.Sc. Thesis, Cairo, Egypt, 2002.
23. O. Morgan and M. Monthly: *Rev. Am. Electroplaters Soc.,* 1947, *34,* p. 41.
24. I. Reich and F.D. Snell: *Ind. Eng. Chem.,* 1948, *40,* p. 37.
25. S. Spring, H.I. Forman, and L.F. Peal: *Ind. Eng. Chem.,* 1946, *18,* p. 4.
26. A.L. Fredrick: *Electroplating,* American Electrochemical Platers' Society, New York, NY, 1978.
27. G.R. Palin: *Electrochemistry for Technologists,* Pergamon Press, New York, 1969.
28. G. Juve and A. Politti: *J. Less-Common Metals,* 1978, *59,* p. 175.
29. J.M. Albella, J. Motero, and J.M. Duart: *J. Electrochim. Acta,* 1987, *32,* p. 255.
30. J.M. Albella, J. Motero, and J.M. Duart: *J. Electrochem. Soc.,* 1985, *132,* p. 814.